

# Do local analogs of Lyman Break Galaxies exist?

R. Scarpa

*Instituto de astrofísica de Canarias, Spain*

riccardo.scarpa@gtc.iac.es

R. Falomo

*Padova Observatory, Italy*

renato.falomo@oapd.inaf.it

and

E. Lerner

*Lawrenceville Plasma Physics, Inc., USA*

elerner@igc.org

## ABSTRACT

The optical properties of a number of supercompact ultraviolet luminous galaxies (UVLG), recently discovered in the local Universe matching GALEX and Sloan Digital Sky Survey (SDSS) data, are discussed. Detailed re-analysis of the SDSS data for these and other similar but nearer galaxies shows that their surface brightness radial profile in both R and u bands is in most cases well described by an extended disk plus a central unresolved component (possibly a bulge). Since the SDSS pipeline used a single disk component to derive the half light radius of these UVLGs their size was severely underestimated. Consequently, the average UV surface brightness is much lower than previously quoted casting doubts on the claim that UVLGs are the local analogs of high redshift Lyman break galaxies.

*Subject headings:* galaxies: general

## 1. Introduction

Lyman Break Galaxies (LBGs; Steidel et al. 1999) are high redshift galaxies thought to be undergoing intense star formation. These galaxies are characterized by compact structure and extremely high surface brightness ( $> 10^9 L_{\odot} \text{ kpc}^{-2}$ ) and have been suggested to be the precursors of present-day elliptical galaxies (see e.g., Giavalisco 2002). While LBGs are rather common at  $z > 2.5$ , it remains unclear whether local analogs of these interesting objects do exist.

In a recent letter by Heckman et al (2005), with details given in Hoopes et al. (2006; Paper 1 & 2 hereafter), the finding in the local Universe ( $z < 0.3$ ) of supercompact UV luminous

( $L_{1530} > 2 \times 10^{10} L_{\odot}$ ) galaxies that share the properties of high redshift LBGs (having UV surface brightness above  $10^9 L_{\odot} \text{ kpc}^{-2}$ ) was reported. These galaxies were identified using data from the GALEX AIS survey (Martin et al. 2005) and Sloan Digital Sky Survey (SDSS) third data release (Abazajian et al. 2005). In particular, 33 galaxies were identified in paper 1 & 2 as having UV luminosity, size, and surface brightness adequate for being classified as local analogs of LBGs.

In Paper 1 & 2 the far-UV surface brightness of the UVLGs is not directly measured. Instead, the half-light radii measured by SDSS in the u-band are used to estimate the surface area of the far-UV emitting region. Specifically, the UV average sur-

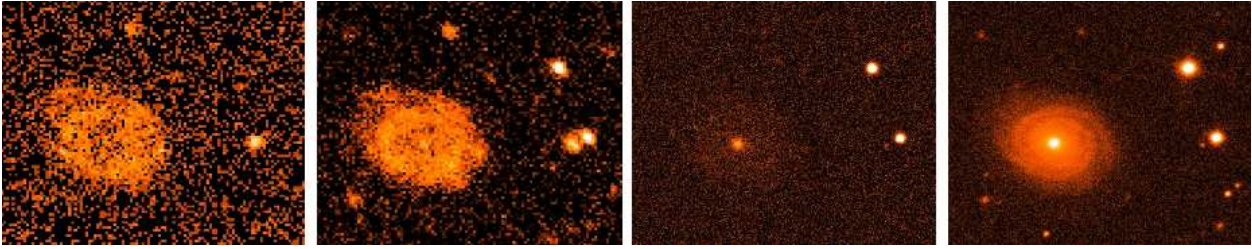


Fig. 1.— From left to right the GALEX far-UV, GALEX near-UV, SDSS  $u$ -band, and SDSS R-band images of a field galaxy located at 02:44:45 -08:09:52 This galaxy was found in the same GALEX image and not far from object 02:45:29 -08:16:37 belonging to the Hoopes list. Note that these are GALEX MIS images, deeper than the AIS images used by Hoopes. The diameter of the disk of the galaxy is approximately 1 arcmin.

face brightness was derived by dividing half the total far-UV flux (from the GALEX archive) by the galaxy surface  $\pi r_e^2$ , where  $r_e$  is the half-light radius from the seeing-corrected exponential model fit calculated by the SDSS pipeline in the  $u$ -band. This procedure yielded 33 supercompact galaxies with far-UV surface brightness  $I_{1530} > 10^9 L_\odot \text{ kpc}^{-2}$ , the alleged LBGs local analogs. For this particular set of galaxies, the half-light radii range from  $0.10 < r_e < 1.04$  arcsec with median value of 0.41 arcsec. It is because of these small radii that the surface brightness is high, the luminosities being in no way exceptional among UVLGs.

It is worth noticing that the quoted  $u$ -band half-light radii (Table 1 in Hoopes et al. 2006) are particularly small being in many cases below 0.3 arcsec. This is much smaller than the typical seeing ( $> 0.8$  arcsec) of SDSS data (Abazajian et al. 2005) and suggests that the SDSS automatic routine used to compute them might have failed. To be more precise, the SDSS pipeline is asked to fit a single disk (exponential) model. In the case of galaxies with two clearly distinct components (the disk and the bulge), this is inappropriate because the algorithm will inevitably tend to fit the central part, the most luminous one, of the surface brightness radial profile. As a result, in a number of cases the half-light radius quoted in the SDSS archive is possibly appropriate for the bulge while missing the faint disk of the galaxy.

Puzzled by this thoughts and given the importance of finding local analogs of LBGs for our understanding of the process of galaxy formation, we were prompted to re-analyzed the SDSS images to check whether the half-light radius in the SDSS

archive provides a reliable measure of the far-UV radii. We shall show that there are good reasons to believe that this is not the case and that the local analogs of LBGs, if they exist at all, have still to be found.

## 2. The Hoopes et al. analysis revisited

To identify in the local Universe the analogs of LBGs both flux and size in the far-UV of candidates are needed. Until recently neither of the two were available for large samples of data. GALEX has provided far-UV (1530 Å) fluxes for thousands of galaxies, allowing the identification of 215 galaxies as luminous as LBGs (Paper 1 & 2). With luminosity at 1530 Å  $L_{1530} > 2 \times 10^{10} L_\odot$ , these galaxies represent the high-luminosity end of the UV luminosity function of non-active galaxies.

While many of the galaxies detected by GALEX are resolved and a direct measure of their UV size is possible, the apparent size of these 215 UV-luminous galaxies is in most cases too small to be resolved. Thus, to estimate their surface brightness the size derived at a different wavelength was used in Paper 1 & 2, under *the assumption that the light distribution does not change significantly between the two bands*. This is a risky assumption, for the UV and optical light distribution in normal galaxies is markedly different. This is nicely illustrated, for instance, in the case of the Andromeda galaxy (Thilker et al. 2005). Another example that allow a quantitative discussion of the SDSS pipeline products is shown in Fig. 1, where we compare the GALEX and SDSS images of a large field galaxy. While in the optical band the emis-

TABLE 1  
HOOPES SAMPLE: FIT TO THE U- AND R-BAND DATA

#	RA	DEC	z	SDSS $r_e$ u-band arcsec	$\log(UV_{SB})$ $L_\odot \text{ kpc}^{-2}$	Best Fit	Core mag	Disk Total mag	Disk $r_e$ R-band arcsec	Corrected $\log(UV_{SB})$ $L_\odot \text{ kpc}^{-2}$	notes
01	01:50:28	13:08:58	0.147	0.65	9.38	PSF+disk	19.2	18.1	1.2	8.84	
02	02:13:48	12:59:51	0.219	0.24	9.92	PSF+disk	18.6	18.4	2.8	7.78	
							19.2	21.5	2.8		
03	01:02:26	14:54:38	0.086	1.04	9.08	disk	*	17.5	1.05	9.07	1
							*	19.4	0.9		
04	00:40:54	15:34:09	0.283	0.40	9.16	PSF	19.8	*	*	8.36	2
05	00:44:47	15:29:11	0.227	0.63	9.04	PSF+disk	19.9	18.8	1.1	8.55	3
							20.1	20.4	1.1		
06	01:51:25	13:25:10	0.243	0.40	9.35	PSF+disk	20.0	19.3	0.8	8.74	
07	02:45:29	-08:16:37	0.195	0.51	9.17	PSF+disk	19.3	19.2	0.8	8.77	3
08	08:17:22	46:44:59	0.280	0.76	9.01	PSF+disk	19.2	20.0	1.3	8.54	4
09	10:51:45	66:06:21	0.170	0.30	9.64	PSF+disk	19.2	19.4	1.2	8.43	
10	13:53:55	66:48:00	0.198	0.58	9.31	PSF+disk	19.0	18.8	0.8	9.03	3
11	09:48:24	61:39:56	0.173	0.35	9.60	PSF+disk	19.1	20.3	0.9	8.78	3
12	10:12:11	63:25:03	0.246	0.32	9.35	PSF+disk	19.2	20.5	2.2	7.67	5
13	08:15:23	50:04:14	0.164	0.66	9.16	PSF+disk	18.7	17.6	1.0	8.79	
14	04:02:08	-05:06:42	0.139	0.49	9.49	PSF+disk	19.0	18.8	1.2	8.71	
							19.9	20.6	1.2		
15	11:39:47	63:09:11	0.245	0.51	9.02	PSF+disk	19.2	19.7	0.9	8.52	
16	09:23:36	54:48:39	0.222	0.32	9.65	PSF+disk	19.6	20.6	1.0	8.66	
17	08:08:44	39:48:52	0.091	0.29	10.20	PSF+disk	17.8	17.9	2.2	8.44	6
							18.2	20.0	2.1		
18	12:39:31	64:41:05	0.133	0.63	9.36	PSF+disk	18.8	18.8	1.1	8.87	7
19	11:33:03	65:13:41	0.241	0.10	10.80	PSF+disk	20.1	20.8	1.0	8.8	
20	20:50:00	00:31:24	0.164	0.21	10.00	PSF+disk	18.8	19.7	1.1	8.56	3
21	23:25:39	00:45:07	0.277	0.25	9.67	PSF+disk	19.9	21.4	1.2	8.30	
22	21:45:00	01:11:57	0.204	0.23	9.82	PSF+disk	18.9	19.5	1.0	8.54	
23	23:07:03	01:13:11	0.126	0.31	9.93	PSF+disk	18.5	19.8	0.9	9.00	8
24	03:28:45	01:11:50	0.142	0.70	9.11	PSF+disk	19.6	18.6	0.9	8.89	
25	09:21:59	45:09:12	0.235	0.41	9.65	PSF+disk	18.6	18.6	1.6	8.46	9
26	09:51:37	48:39:41	0.135	0.79	9.04	PSF+disk	19.7	19.3	0.7	9.14	
27	08:21:37	37:10:46	0.284	0.43	9.47	PSF+disk	19.6	19.3	0.5	9.33	
28	09:26:00	44:27:36	0.181	0.34	9.91	PSF+disk	19.2	19.5	0.7	9.28	
29	09:54:34	51:35:08	0.130	0.67	9.60	PSF+disk	18.5	18.2	0.9	9.34	
30	23:18:12	-00:41:26	0.252	0.61	9.29	PSF+disk	19.3	18.7	1.2	8.70	
							20.3	20.5	1.2		
31	00:10:09	-00:46:03	0.243	0.36	9.37	PSF+disk	20.2	19.6	1.0	8.48	10
							21.1	21.6	1.1		
32	00:55:27	-00:21:48	0.167	0.28	9.89	PSF+disk	18.4	19.9	0.9	8.87	
33	23:53:47	00:54:02	0.223	0.60	9.01	PSF+disk	19.9	20.2	0.7	8.87	

NOTE.—

The first line for each source refers to the R-band data, while when present the second line gives the best fit in the u-band. Uncertainties on best fit parameters in the R-band are  $\pm 0.1$  magnitudes and  $\pm 0.1$  arcsec, or smaller. In the u-band errors are  $\pm 0.1$  magnitudes for the core and  $\pm 0.2$  mag and  $\pm 0.2$  arcsec for the disk.

1: Problem in GALEX image. Source right on the edge of the field of view.

2: Unresolved. To compute the surface brightness the radius was set to 1 arcsec, similar to the atmospheric seeing and equal to the median of the sample.

3: Double.

4: Bad Fit. Core with extremely boxy isophotes and an off-center light pick.

5: Close to bright star.

6: Triple. Also acceptable fit with a de Vaucouleurs law with  $r=1.3$  arcsec.

7: Object right on-top of the diffraction figure of a nearby bright star. The shape of the low intensity isophotes is strongly affected by this diffuse light in the north-east side of the galaxy.

8: Elongated, possibly double.

9: Head-tail morphology. Possibly embedded companion at 1.2 arcsec.

10 Head-tail morphology. Possibly embedded companion at 0.9 arcsec.

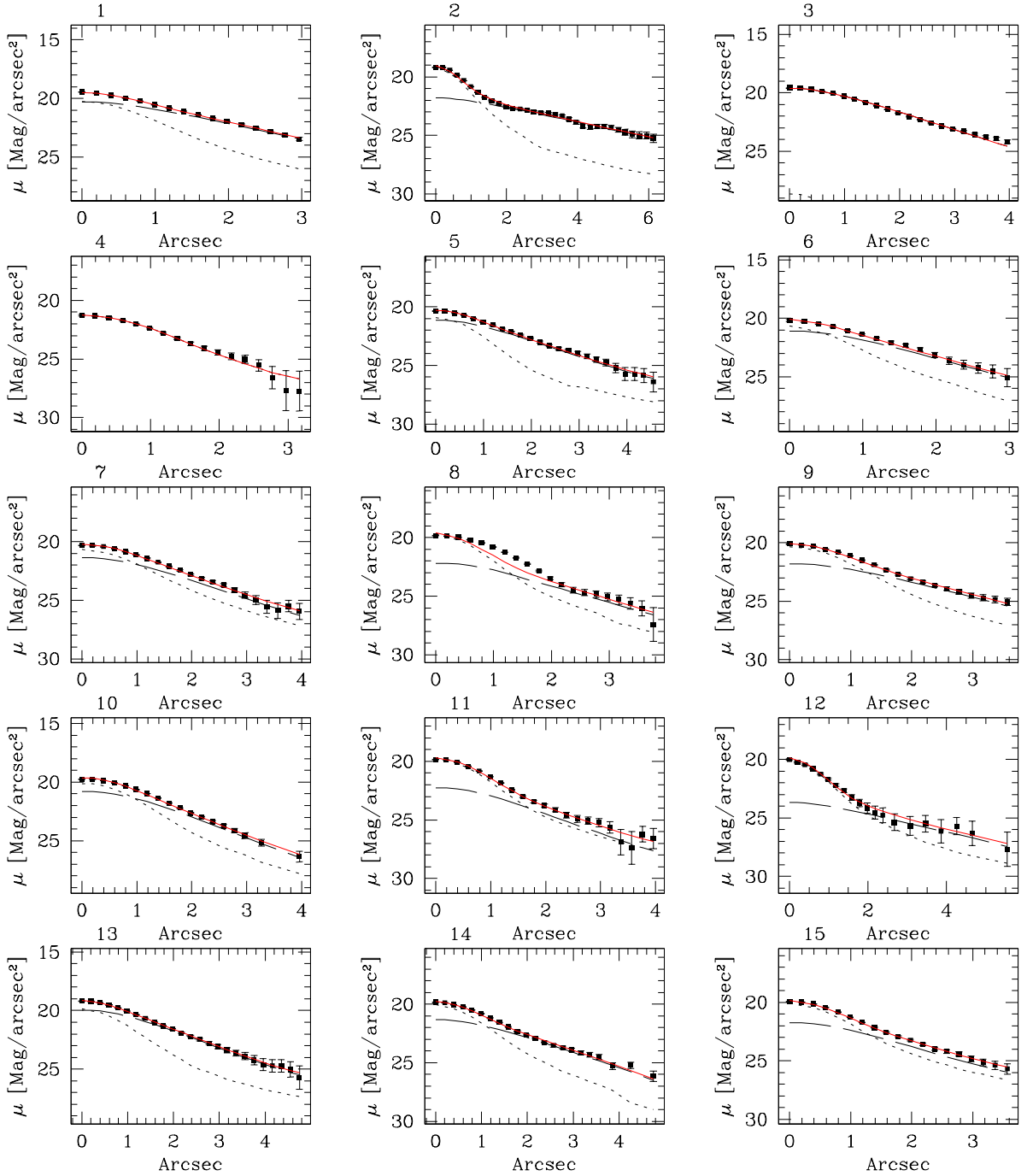


Fig. 2.— Best fit of the average R-band surface brightness radial profile (points with error bars) for all object in Table 1. The observed radial profile is shown by the points with errorbars. The PSF model is shown by a dotted line, while the disk model convolved with the PSF is shown by a dashed line. The sum of the two components is shown by the solid line.

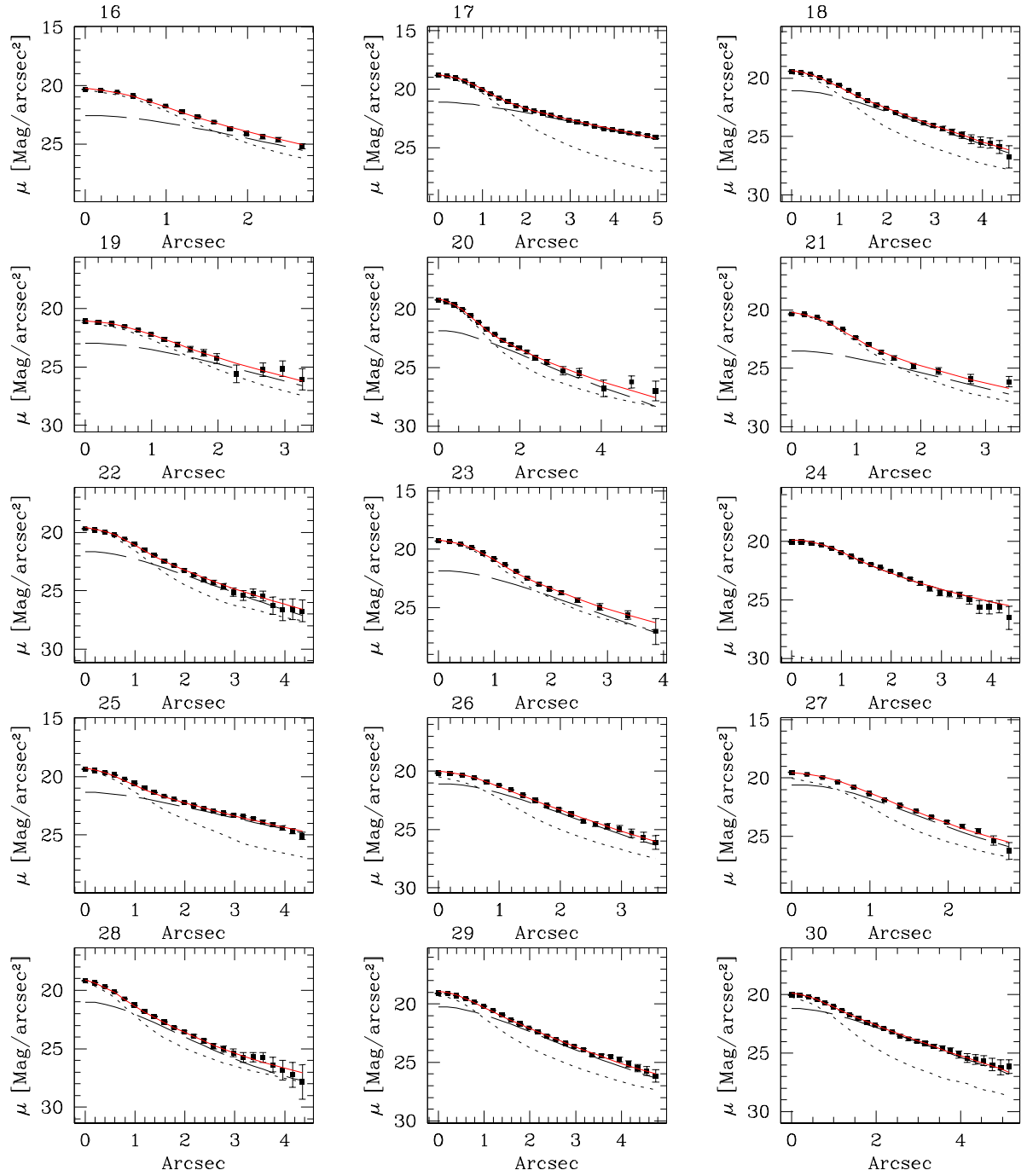


Fig. 2.— Continued

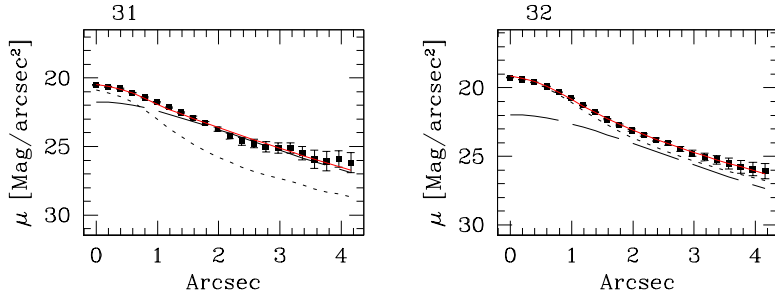


Fig. 2.— Continued

sion is dominated by the central bulge, in the UV there is almost no light coming from the center. Moreover, in the shallower u-band image (in the Sloan survey the exposure time is the same for both the u and R bands), the disk of the galaxy is mostly undetected. In these two images the SDSS pipeline fits two completely different light distributions, yielding best fit exponential models with  $r_e = 2.4$  and  $12.9$  arcsec in the u and R bands, respectively. Applying the procedure followed in Paper 1 & 2 the UV surface brightness is overestimated by almost 30 times. Clearly, in the u-band the pipeline has fitted only the central core of the galaxy while the UV emission comes from the extended disk. We learn here that (a) the deeper R-band image should be preferred to characterize the optical size of the galaxy, (b) the UV and optical size of the *disk* is basically the same, and (c) if a prominent bulge exists a single component fit is inappropriate even to describe the optical data, let alone the far-UV.

Thus, we retrieved from the SDSS archive the raw images for all the 33 objects reported as having surface brightness above  $10^9 L_\odot \text{ kpc}^{-2}$  in the Hoopes et al. list, and re-analyze the average surface brightness profile extracted from both the u- and R-band images allowing for the presence of multi-components. The fitting procedure was as follow. First, for each object a model of the PSF was created averaging the radial profile of a number of bright stars in the same frame of the object. Then this model was used to convolve the galaxy profile, either an exponential (disk) or a de Vaucouleurs law. The best fit was then determined

by chi-squared minimization. With only two exceptions, it was found that the surface brightness radial profile extracted from the R-band data is well described as the sum of a central unresolved point source, possibly the bulge of the galaxy, plus an extended disk. Results are given in Table 1 and Figure 2. In no case could a de Vaucouleurs law give better results than a disk model. Object # 3 is the only one for which we can reproduce the SDSS fit with a single disk and no central component. In one case (object # 4) because of the poor atmospheric seeing (1.5 arcsec) the source is found fully consistent with the PSF profile and therefore the half-light radius quoted in the SDSS archive is meaningless.

The u-band data are considerably shallower than the R-band data. Because of this only in seven cases the disk is large and bright enough to be detected also in the u-band. Results of the best fit are reported in Table 1 (second entry for each object) and shown in Fig. 3. The surface brightness profile of the remaining 26 sources is dominated by the unresolved core while the disk is virtually undetected. As a consequence, objects are either unresolved or marginally resolved and the half-light radius derived by the SDSS pipeline is highly uncertain as already pointed out in Paper 1 & 2. As a whole we see that in all cases where a comparison is possible, the best fit models from the two bands are fully consistent with each other directly showing that the light distribution in the two bands is very similar and either of the two can be used to characterize the structure of the object.

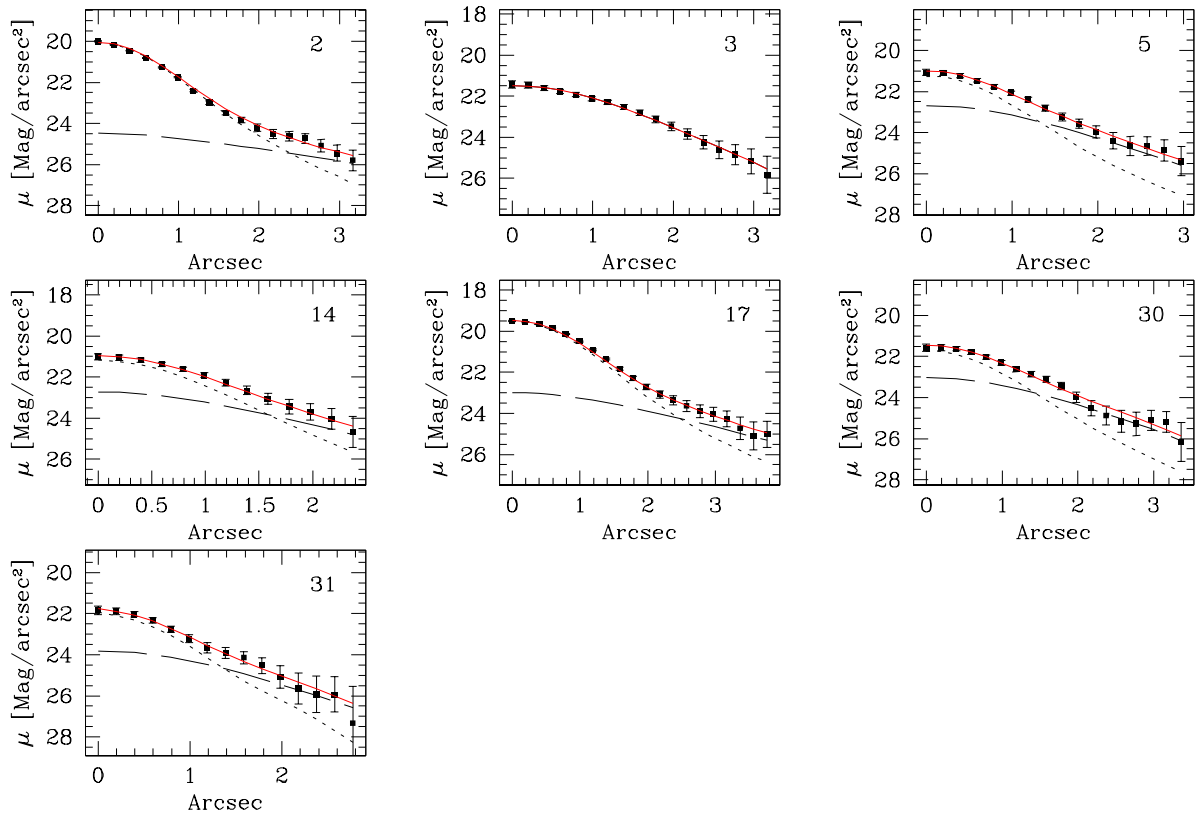


Fig. 3.— Best fit of the average u-band surface brightness radial profile for the brighter disks. Symbols as in figure 4. Best fit parameter are in Table 1.

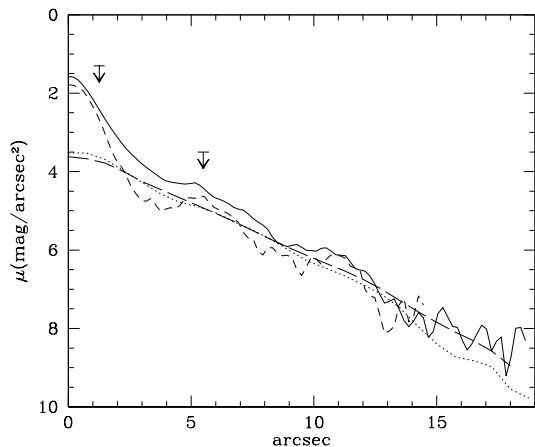


Fig. 4.— Comparison of the average surface brightness radial profiles from various bands for the galaxy at 232207.9–000314 (last entry in Tab. 2). Profiles were stacked one on the other (the flux scale is arbitrary) to evidentiate the similarities at large radii. Different lines show the R-band (solid), the u-band (dashed), near-UV (dotted), and far-UV (long dashed) profiles. The emission from the bulge component is dominant in u- and R-band up to  $\sim 3$  arcsec, while it is negligible in the UV. The disk is detected and has the same scale length of 5.5 arcsec (6 kpc) in all four bands. The two arrows indicate the u-band and far-UV half-light radii.

### 3. Discussion

We have shown that the surface brightness profile of these 33 supercompact UVLGs cannot be described by a single disk model. This result has important implications for their identification as LBGs analogs in the local Universe.

When studying high- $z$  LBGs the half-light radius – not the scale length of the disk – is used to compute their far-UV average surface brightness. Due to the high redshift of LBGs, the rest frame far-UV emission is directly accessible in the optical band with adequate resolution and thus both luminosity and size are derived at the same wavelength.

The use of the half-light radius then provides a model independent measure of the average surface brightness. On the other hand, in the case of UVLGs the situation is different because due to the low spatial resolution of GALEX one has to use luminosities and radii from two different bands and the use of the half-light radius might not be adequate. The problem is serious indeed because our re-analysis of the R-band and u-band data of all the 33 alleged supercompact UVLGs has shown that most of these galaxies cannot be described with a single disk model. Instead, we found a significant fraction of their total flux is due to an unresolved core, most probably the bulge. In normal nearby galaxies stars belonging to the bulge do not contribute significantly to the far-UV emission. It is from the disk that most of the far-UV radiation comes from (see discussion above). Thus to describe the far-UV light distribution starting from data taken in the optical band it seems appropriate to use the scale length of the extended disk – not the half-light radius of the whole object – in order to isolate and remove the bulge component.

Now the question remains of whether this result, valid for normal galaxies, is also applicable to supercompact UVLGs that are peculiar in a number of ways. To investigate this point we searched the GALEX medium imaging survey (MIS) archive to find nearby, non-interacting, resolved (having stellarity<sup>1</sup>  $< 0.45$  and half light radius  $> 4.5$  arcsec) SDSS galaxies for which a direct measurement of the far-UV surface brightness can

<sup>1</sup>The stellarity index is produced by the SExtractor program and differentiates galaxies from unresolved objects



be obtained.

We further selected objects with color  $(u-R) < 1.0$ , as is the case for most objects in the Hoopes sample, and far-UV luminosity above  $10^{10} L_{\odot}$ . This resulted in only 4 galaxies (Table 2) with color and luminosity comparable to the one of supercompact UVLGs but close enough to be resolved by GALEX. In all four cases the u-band half-light radius as derived by the SDSS pipeline is significantly smaller than that in the far-UV. In particular, two of them are quite compact in the u-band and their far-UV surface brightness (as estimated by the Hoopes method) is brighter than  $10^9 L_{\odot}/\text{kpc}^2$ . Therefore they are borderline examples of the supercompact UVLGs.

In reality, the direct measurement of the far-UV half-light radius show that both galaxies are quite large and their far-UV surface brightness is below  $8 \times 10^7 L_{\odot} \text{ kpc}^{-2}$ . The reason for this systematic difference between far-UV and u-band size is the different distribution of the stars emitting in the two bands. In the u-band stars from both the disk and the bulge contribute to the observed luminosity, while virtually only the stars in the disk contribute to the far-UV emission (Fig. 4). Thus when galaxies like those of the Hoopes sample, but merely closer, are observed, the u-band half light radius is typically far smaller than the far-UV radius.

We conclude that the optical scale length of the extended disk – not the half-light radius used in paper 1 & 2 – provides the best, though imperfect, description of the far-UV light distribution. This implies that the size of the far-UV emitting region is much larger than the value used by Hoopes, with radii ranging from 0.5 to 2.8 arcsec, with median of 1.0 arcsec. On average this is a factor 2.5 larger than the values used by Hoopes et al., corresponding to a reduction of 6.25 times of the surface brightness. The most dramatic changes, up to two orders of magnitude, occur for the objects with the smaller radii as according to our analysis all objects with radius smaller than 0.4 arcsec are gone. As a whole our estimate of the far-UV surface brightness (Tab. 1) is below the threshold for classifying these objects as supercompact UV luminous galaxies (Fig. 5). The present data therefore do not support the claim of the existence in the local universe of galaxies with properties similar to the one of high redshift LBGs.

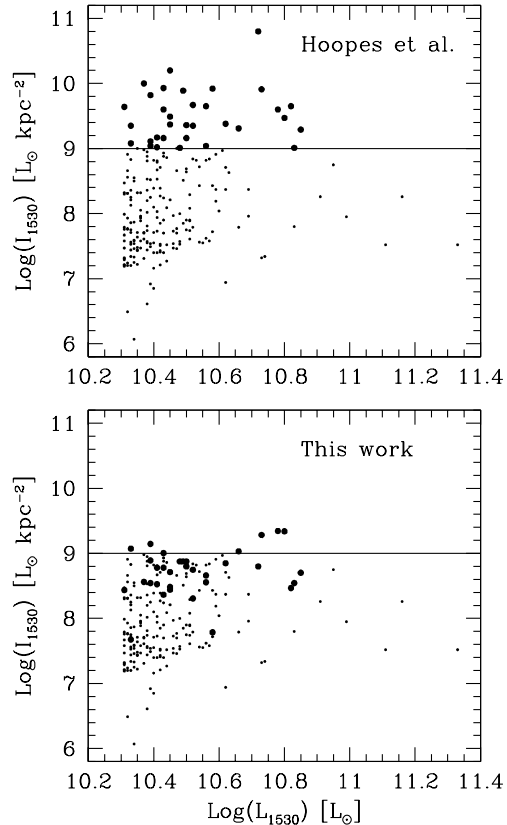


Fig. 5.— **Upper panel:** Distribution in the luminosity – surface brightness plane of the 215 UV luminous galaxies reported by Hoopes et al. According to Hoopes et al. the region of LBGs, above  $\log(I_{1530}) > 10^9 L_{\odot} \text{ kpc}^{-2}$ , is populated by 33 objects (big dots). **Lower panel:** Same as above but using our revised surface brightness of the alleged 33 LBGs analog (big dots). In this case the LBGs region is almost empty.

TABLE 2  
THE BLUE SAMPLE OF GALAXIES

RA	DEC	z	$m_{FUV}$	$m_u$	$r_{FUV}$	$r_u$	(u-R)	$\log L_{FUV}$	$\log \Sigma_u$	$\log \Sigma_{FUV}$
085625.2	513148	0.083	19.3	18.6	4.64	3.63	0.98	10.1	7.75	7.54
090031.0	552208	0.076	19.2	19.8	4.69	0.84	0.88	10.0	9.06	7.57
143753.8	050046	0.087	19.2	18.1	5.31	3.00	0.85	10.1	7.93	7.43
232207.9	-000314	0.057	17.9	17.8	6.02	1.26	0.92	10.3	9.20	7.84

NOTE.—Columns give: Right ascension and Declination for the 2000 equinox; (3) redshift; (4) far-UV magnitude as from GALEX archive; (5) Petrosian u-band magnitude from SDSS archive; (6) far-UV half light radius from GALEX archive in arcsec; (7) u-band SDSS effective radius from the seeing-corrected exponential model fit in arcsec; (8) (u-R) color in magnitudes; (9) far-UV luminosity in solar units; (10) Average surface brightness derived from  $r_u$ , in  $L_\odot \text{ kpc}^{-2}$ ; (11) true far-UV surface brightness derived from  $r_{FUV}$ , in  $L_\odot \text{ kpc}^{-2}$ .

*Facilities:* GALEX, SDSS, HST (MUST archive).

## REFERENCES

- Abazajian, K., et al. 2005, AJ, 129, 1755
- Giavalisco, M. 2002, ARA&A, 40, 579
- Heckman T.M., Hoopes C.J., Seibert M., et al. 2005, ApJ, 619, L35; Paper 1
- Hoopes, C.J., Heckman T.M., Salim S., et al. 2006 ApJS in press, (astro-ph/0609415); Paper 2
- Martin, D. C., et al. 2005, ApJ, 619, L1
- Steidel, C. C., Adelberger, K. L., Giavalisco, M., Dickinson, M., & Pettini, M. 1999, ApJ, 519, 1
- Thilker, D. A., Hoopes, C. G., Bianchi, L. et al. 2005, ApJ 619, L67